



OPEN

Molecular characteristics and expression pattern of the *FAR1* gene during spike sprouting in quinoa

Liubin Huang^{1,2}, Lingyuan Zhang^{1,2}, Ping Zhang¹, Junna Liu¹, Li Li¹, Hanxue Li¹, Xuqin Wang¹, Yutao Bai¹, Guofei Jiang¹ & Peng Qin¹✉

FAR-RED IMPAIRED RESPONSE 1 (FAR1) is a class of transposase-derived transcription factors that play a very important role in the initiation of the photosensitive pigment A (phyA) signaling pathway. Despite their importance, the understanding of the function of *FAR1* genes in quinoa is still limited, especially regarding how they affect the spike sprouting response. Quinoa has gained global attention in recent years for its health benefits and potential for sustainable agriculture. In our study, the *CqFAR1* gene set in quinoa was characterized using HMMER (PF03101) and BLAST analyses, and 87 genes were identified. The 87 *CqFAR1* genes were systematically classified into five groups that showed a high degree of conservation in gene structure and motif composition. Tissue expression profiles of the *CqFAR1* gene indicated that the *CqFAR1* gene plays a key role throughout the growth and development of quinoa, especially at mid (leaf) and end (spike) stages. By RT-qPCR analysis, we observed significant differences in the expression of the *CqFAR1* gene at different developmental stages. Notably, the *CqFAR1* gene showed significant expression enhancement at the early stage of quinoa spike sprouting. The results are useful for understanding the role of the *CqFAR1* gene in quinoa growth and development and provide theoretical support for quinoa breeding.

Keywords *Chenopodium quinoa*, *FAR1*, Spike sprouting, Expression profiling

FAR-RED IMPAIRED RESPONSE 1 (FAR1) is derived from a family of homologous proteins of transposases, originally identified in the model plant *Arabidopsis thaliana* as an important component of the photoreceptor pigment A (phyA)-mediated far-red-light signaling pathway, and belongs to a family of transcription factors that are found in most angiosperms^{1,2}. The FAR1 protein contains three main functional structural domains: the N-terminal C2H2 zinc finger structural domain with DNA-binding activity; the central possible core transposase structural domain; and the C-terminal SWIM zinc finger structural domain, which has a transcriptional activation function³. In addition, the *FAR1* gene family plays various important roles in plant physiology and development, including participation in light signaling responses⁴, various stress responses⁴, regulation of chlorophyll biosynthesis⁵, ABA signaling⁶, regulation of the biological clock and flowering time⁷, and other key processes. In terms of light signaling response, the *FAR1/FHY3* dimer directly binds to the promoter. It activates the expression of two key regulators, *FHY1* and *FHL*, which are key regulators of nuclear translocation, thus indirectly affecting the nuclear translocation process of PhyA⁸. During plant growth and development, dimers formed by *FAR1* and *FHY3* promote the expression of the ARC5 promoter by directly binding to it, thereby activating the synthesis of a dynamin protein essential for chloroplast division⁹. In addition, *FHY3* and *FAR1* can participate in the regulation of starch synthesis by promoting the transcriptional activation of *ISA2*, which in turn regulates starch synthesis induced by daytime light¹⁰. Particularly importantly, disruption of *FHY3* and *FAR1* expression significantly attenuated the inhibitory effects of ABA on seed germination, seedling greening, and root elongation processes⁶. In addition, they can bind to the *ABI5* promoter and promote its transcriptional activity, which in turn participates in the ABA signaling process⁶. So far, the *FAR1* gene family has been analyzed and reported in many plant species. For example, in *Arabidopsis thaliana*¹¹, *Arachis hypogaea*¹², *Zea mays*¹³, and *Solanum tuberosum*¹⁴, 12, 24, 16, and 20 *FAR1* family members were found respectively. However, there is no research on the analysis of the *FAR1* gene or the whole gene family in quinoa. Therefore, it is necessary to further study the function of *CqFAR1* gene family members.

¹Present address: College of Agronomy and Biotechnology, Yunnan Agricultural University, Kunming 650201, China.

²These authors contributed equally: Liubin Huang and Lingyuan Zhang. ✉email: wheat-quinoa@ynau.edu.cn

After a long domestication process, most crops have lost their inherent dormancy characteristics¹⁵. Under the continuous rainy or humid conditions before harvest, seeds are easy to germinate prematurely on the mother plant, which is called spike sprouting¹⁶. Spike sprouting usually severely reduces crop yield and quality¹⁷. According to statistics, the global grain loss caused by spike sprouting is more than 1 billion US dollars every year. In order to effectively reduce yield loss, it is very important to study the genetic basis of seed dormancy and spike sprouting.

Quinoa (*Chenopodium quinoa* Willd.), commonly known as "fake grain," is a dicotyledonous plant under Amaranthaceae, with the characteristics of tetraploid ($2n=4x=36$) C3 crops. It has a common history of more than 8000 years with the Andean indigenous culture and is honored as the "mother of ten thousand valleys" for its unparalleled nutritional and cultural value^{18–21}. It is especially suitable for quinoa planted in alpine mountainous areas. Its maturity coincides with the rainy season, which easily causes spike sprouting, which will not only seriously affect the yield and quality of quinoa, but also reduce its commodity value and market competitiveness. However, research on the mechanism of seed dormancy and spike sprouting is relatively scarce, which largely limits the process of quinoa breeding. Therefore, it is very important to determine whether the *FAR1* gene plays a role in seed dormancy and spike sprouting of quinoa.

In this study, we screened and identified the *CqFAR1* gene family using the quinoa genome, analyzed its gene structure, phylogenetic relationships, GO functional annotation, and chromosomal localization, and performed expression pattern analysis based on the expression data of this family of genes in quinoa, as well as analyzed the promoter cis-acting elements. In addition to light-responsive elements, the quinoa *FAR1* gene also contains abundant hormone-responsive elements and growth and developmental elements. We investigated the expression trends of the *CqFAR1* gene at different times and initially discussed the expression patterns of these family members under spike sprouting, to provide theoretical references and bases for subsequent functional studies and applications of the *CqFAR1* gene in quinoa.

Results and analysis

Identification and physicochemical properties of *CqFAR1* gene family members

A total of 87 *CqFAR1* genes were identified from the quinoa genome (Table 1), and the protein sequence length encoded by the genes ranged from 138 to 1,051 amino acids, with an average protein length of 526 amino acids. The molecular weight ranged from 16,702.1 kDa to 121,696.35 kDa, and the average molecular weight was 60,470.21 kDa. *AUR62033390* had the largest protein length and molecular weight, while *AUR62026577* had the smallest. The isoelectric point is between 4.71 and 9.62, and the average isoelectric point is 7.04. The instability coefficient of most proteins was > 40 , indicating that they were unstable proteins. The fat index ranged from 55.68 to 85.23, and the average fat index was 70.81. The total average hydrophilicity is < -0.2 . According to the Protscale function in ExPASY, it is known that all proteins are hydrophilic proteins. In addition, the subcellular localization predicted that most of *CqFAR1* was located in the nucleus, cytoplasm, and chloroplast, while only *AUR62008862* was located in the cytoskeleton, and *AUR62017651* was located in the peroxisome.

Phylogenetic analysis of *CqFAR1* genes

To deeply analyze the evolutionary relationship of the *CqFAR1* gene family in quinoa, we constructed an unrooted phylogenetic tree based on the *FAR1* protein sequences of *C. quinoa*, *O. sativa*, and *A. thaliana*. The *CqFAR1* gene could be categorized into five main subgroups. The class I subfamily contains 18 genes, including 1 *C. quinoa* gene, 1 *O. sativa* gene, and 16 *A. thaliana* genes; there are 4 class II genes, including 0 *C. quinoa* genes, 2 *O. sativa* genes, and 2 *A. thaliana* genes; class III genes only contain 8 *C. quinoa* genes; there are 126 class IV genes, including 60 *C. quinoa* genes, 17 *O. sativa* genes, and 49 *A. thaliana* genes; there are 130 class V genes, including 18 *C. quinoa* genes, 44 *O. sativa* genes, and 68 *A. thaliana* genes (Fig. 1). These data show that the closer the phylogenetic relationship of family members, the higher the similarity of gene structure and domain. Further analysis suggested that different subtypes of *FAR1* genes may assume different biological functions and genes with similar structures may play a related role in the regulation of growth and development of quinoa.

Conservative domain, gene structure and visual analysis of *CqFAR1* protein

The composition and distribution of motifs are relatively conserved among members of the same subpopulation, and motifs between different subpopulations may lead to differences in *CqFAR1* gene function (Fig. 2a). Motif 1 exists in all protein sequences. Motif 2 and Motif 3 are located at the N-terminal of most *CqFAR1* protein sequences. The motif types and numbers of the same subgroup are similar, indicating that the motif pattern may be related to the function of the *CqFAR1* protein. The conserved domain analysis of *CqFAR1* protein using TBtools-II (v2.119) software showed that most genes belonged to the *FAR1* superfamily and *FHY3* superfamily. Only *AUR62036755* had the *DBD_Tnp_Mut* superfamily, *AUR62023657* had *DUF4283*, *AUR62017462* had *OTU_plant_OTU9-like*, *AUR62008862* had the *FBD* superfamily, and *AUR62042833* had the *MULE* superfamily. These results showed that the structure of the *CqFAR1* gene was diverse (Fig. 2b). To further understand the distribution of *CqFAR1* exons and introns, clarify the inherent sequence diversity of the *CqFAR1* gene family, and analyze its exon and intron distribution and cross-species conservation, the results showed that the number of exons in *CqFAR1* genes ranged from 1 to 16. It is worth noting that *AUR62024057* has only one exon, and *AUR62017462* has 16 exons. The CDS of most *CqFAR1* genes is not interrupted by introns. Although there are differences in the location of exons, the *CqFAR1* gene family members clustered in the same phylogenetic branch usually have similar or the same number of exons (Fig. 2c).

Chromosomal localization and gene duplication of *CqFAR1* genes

Chromosomal localization results showed that the *CqFAR1* gene family was distributed on all chromosomes except chromosome 13. Among them, the number of *CqFAR1* genes on chromosome 17 and chromosome 1

Gene ID	Protein length	Mw (kDa)	pI	Instability index	Aliphatic index	GRAVY	Subcellular localization
AUR62001611	825	93,172.71	7.57	46.45	74.00	-0.424	Nucleus
AUR62002320	499	57,258.63	8.94	45.62	75.75	-0.578	Nucleus
AUR62002424	685	79,335.84	6.13	46.68	85.23	-0.269	Nucleus
AUR62003534	795	91,634.24	6.92	56.97	69.69	-0.634	Nucleus
AUR62003731	776	90,529.21	6.55	44.23	67.60	-0.752	Nucleus
AUR62003777	389	44,744.33	6.83	46.49	55.68	-0.997	Nucleus
AUR62003863	597	69,785.67	9.31	40.67	68.63	-0.587	Nucleus
AUR62003871	813	93,654.91	6.26	44.84	71.51	-0.567	Nucleus
AUR62003900	365	41,980.72	5.31	44.85	68.85	-0.711	Nucleus
AUR62004004	446	51,370.72	7.31	41.19	65.31	-0.831	Nucleus
AUR62006821	776	91,135.97	6.29	43.59	67.36	-0.756	Nucleus
AUR62006830	656	76,298.82	8.72	46.92	66.17	-0.571	Nucleus
AUR62008235	818	95,570.68	6.13	44.34	66.75	-0.780	Nucleus
AUR62008862	327	37,823.60	5.99	57.72	75.11	-0.693	Cytoskeleton
AUR62009197	317	36,081.23	5.25	48.37	76.88	-0.686	Cytoplasm
AUR62009336	412	47,584.34	6.96	39.59	64.56	-0.877	Nucleus
AUR62009774	569	65,596.85	6.57	57.92	69.10	-0.642	Nucleus
AUR62011505	620	71,950.34	4.91	44.32	73.69	-0.589	Nucleus
AUR62011506	647	74,992.73	8.70	47.97	82.12	-0.427	Nucleus
AUR62013200	645	73,435.08	6.23	48.56	75.88	-0.484	Nucleus
AUR62013877	712	82,545.91	6.13	40.41	67.11	-0.734	Nucleus
AUR62013882	227	26,967.77	8.83	57.41	66.96	-0.858	Cytoplasm
AUR62014678	369	41,285.99	9.09	48.29	71.38	-0.735	Nucleus
AUR62014696	420	48,424.96	9.62	36.34	67.74	-0.959	Nucleus
AUR62015251	184	20,701.16	5.98	47.08	58.75	-0.679	Cytoplasm
AUR62016321	621	72,149.63	4.95	43.53	74.06	-0.592	Nucleus
AUR62016322	560	65,297.19	8.72	47.96	79.04	-0.554	Nucleus
AUR62017439	694	79,465.62	7.29	46.97	82.46	-0.306	Nucleus
AUR62017462	782	89,060.78	8.30	44.28	66.68	-0.567	Nucleus
AUR62017476	403	46,181.89	8.99	56.68	67.49	-0.803	Nucleus
AUR62017651	445	52,414.83	5.35	39.60	68.97	-0.834	Peroxisome
AUR62017759	459	52,920.31	6.78	41.23	64.51	-0.850	Nucleus
AUR62019840	469	54,096.50	8.48	56.29	67.55	-0.778	Nucleus
AUR62019926	424	48,700.19	5.29	39.45	69.15	-0.670	Cytoplasm
AUR62020169	740	83,310.52	6.68	50.00	76.80	-0.385	Nucleus
AUR62020476	636	72,430.27	6.72	51.16	70.36	-0.633	Nucleus
AUR62020737	356	40,872.25	5.19	49.05	66.77	-0.761	Nucleus
AUR62023657	624	70,725.15	9.16	35.28	66.62	-0.648	Nucleus
AUR62023864	427	48,799.44	7.99	45.10	72.32	-0.752	Nucleus
AUR62024057	184	20,680.79	9.30	24.34	65.65	-0.603	Nucleus
AUR62024627	263	30,707.43	6.15	45.48	66.31	-0.998	Nucleus
AUR62025742	349	39,968.48	8.90	35.57	74.01	-0.746	Nucleus
AUR62025986	445	51,056.26	6.54	38.72	66.34	-0.804	Nucleus
AUR62026577	138	16,702.10	8.78	64.65	64.93	-0.808	Cytoplasm
AUR62027644	247	28,077.21	4.78	43.32	76.23	-0.621	Cytoplasm
AUR62029067	384	44,243.47	8.12	41.56	75.65	-0.425	Cytoplasm
AUR62029102	685	79,153.74	6.29	46.94	85.09	-0.243	Nucleus
AUR62029711	679	77,871.35	6.02	50.60	67.98	-0.694	Nucleus
AUR62030115	448	52,599.95	6.71	46.68	69.20	-0.476	Cytoplasm
AUR62030618	747	86,560.88	6.25	48.36	68.70	-0.627	Nucleus
AUR62032468	694	79,679.82	6.88	47.65	83.44	-0.302	Nucleus
AUR62033098	423	47,626.19	8.42	57.48	69.53	-0.481	Nucleus
AUR62033390	1051	121,696.35	5.76	44.36	73.47	-0.577	Nucleus
AUR62033700	459	51,883.76	6.70	42.67	70.87	-0.627	Nucleus
AUR62033960	767	89,005.85	6.19	48.55	70.68	-0.577	Nucleus

Continued

Gene ID	Protein length	Mw (kDa)	pI	Instability index	Aliphatic index	GRAVY	Subcellular localization
AUR62034038	549	64,337.45	8.42	41.74	69.64	-0.490	Nucleus
AUR62034337	621	70,666.31	8.86	44.54	71.35	-0.571	Cytoplasm
AUR62035065	754	85,705.52	5.98	51.91	80.09	-0.330	Nucleus
AUR62035513	260	29,305.09	5.65	39.16	65.50	-0.650	Cytoplasm
AUR62035717	624	72,448.59	8.86	47.18	67.24	-0.567	Nucleus
AUR62036316	407	47,270.77	8.59	38.88	68.99	-0.530	Cytoplasm
AUR62036643	394	45,273.79	5.81	30.51	66.50	-0.726	Cytoplasm
AUR62036664	636	73,820.30	5.54	42.15	70.39	-0.540	Nucleus
AUR62036716	674	77,751.86	6.22	28.05	66.53	-0.594	Nucleus
AUR62036755	1023	115,652.59	6.23	36.46	75.06	-0.492	Cytoplasm
AUR62037106	365	40,742.70	9.30	48.92	70.19	-0.574	Nucleus
AUR62037552	666	77,133.26	8.91	32.99	66.29	-0.586	Nucleus
AUR62037793	337	38,071.90	8.25	46.67	76.85	-0.378	Cytoplasm
AUR62038308	586	68,610.61	5.08	47.39	68.21	-0.770	Nucleus
AUR62039220	657	75,950.34	5.88	58.89	70.97	-0.621	Nucleus
AUR62039343	457	52,097.69	9.00	42.56	78.88	-0.511	Cytoplasm
AUR62039824	459	52,921.30	6.65	40.65	64.73	-0.859	Nucleus
AUR62040034	265	30,282.72	5.21	50.37	73.92	-0.770	Nucleus
AUR62040076	587	67,480.17	7.00	36.34	66.61	-0.597	Nucleus
AUR62041272	619	69,408.48	8.05	46.03	67.50	-0.590	Chloroplast
AUR62041424	359	41,036.18	9.15	42.68	65.13	-0.726	Nucleus
AUR62042021	294	33,410.17	9.13	38.52	73.27	-0.736	Nucleus
AUR62042129	241	26,782.27	5.19	29.74	71.12	-0.498	Nucleus
AUR62042190	451	52,945.38	7.91	46.74	68.58	-0.505	Cytoplasm
AUR62042615	661	76,805.57	5.79	43.59	67.59	-0.569	Nucleus
AUR62042707	518	59,912.95	5.96	48.29	65.87	-0.863	Nucleus
AUR62042792	367	41,808.57	5.50	41.00	70.90	-0.708	Nucleus
AUR62042833	403	45,409.73	9.50	52.56	76.58	-0.522	Chloroplast
AUR62042947	770	87,650.82	6.08	51.35	82.22	-0.306	Nucleus
AUR62043517	258	29,454.47	4.71	57.35	68.76	-0.803	Cytoplasm
AUR62043574	672	76,208.20	6.32	50.95	82.62	-0.269	Chloroplast
AUR62044420	320	36,751.97	5.23	48.01	69.75	-0.758	Cytoplasm

Table 1. Physicochemical properties of the quinoa *FAR1* gene family.

was the most (12 and 9, respectively), while the number of *CqFAR1* genes on chromosomes 8, 12, and 14 was the least, with only one *CqFAR1* gene. In other chromosomes, there are 8 *CqFAR1* genes on chr00, 4 genes on chr06, 8 genes on chr09, 2 genes on chr10, 4 genes on chr11, 3 genes on chr02, chr04 and chr15, 6 genes on chr03, chr07 and chr16, and 5 genes on chr05 and chr18. *CqFAR1* genes on some chromosomes tend to exist in clusters, such as *AUR62003731*, *AUR62003777*, *AUR62003863*, *AUR62003871* and *AUR62003900*, which are closely adjacent in physical position. On the whole, *CqFAR1* genes tend to be located at the bottom of the chromosome, followed by the top, and the middle region is less populated. In addition, most *CqFAR1* genes tend to be located in chromosome regions with high gene density (Fig. 3a). Gene duplication plays an important role in the evolution of organisms. The replicated genes lay the foundation for the physiological and morphological changes of individual plants. The whole genome of quinoa was analyzed for collinearity. The results are as follows (Fig. 3b). A total of 19 collinearity gene pairs were identified among 87 *CqFAR1* genes. These collinearity gene pairs were scattered across 18 chromosomes of quinoa. There may be a large number of gene duplication events in the evolution of *CqFAR1* family genes. In the quinoa genome, the *CqFAR1* gene family has been amplified to some extent. All these indicate that gene duplication plays a very important role in the evolution of quinoa.

Collinearity analysis of *CqFAR1* gene

Collinearity analysis is an important tool to reveal the process of genome differentiation and evolution. To further study the covariance of the *CqFAR1* gene family, we found a collinear relationship between *CqFAR1* in *C. quinoa*, *O. sativa* and *A. thaliana* (Fig. 4). One pair of *CqFAR1* gene and *OSFAR1* gene had collinearity (*AUR62017462-OS04T0402300-00*), and 10 pairs of *CqFAR1* gene and *AtFAR1* gene had collinearity (*AUR62023864-AT2G43280.1*, *AT3G59470.2*, *AUR62011505-AT1G80010.1*, *AT1G52520.1*, *AUR62016322-AT1G80010.1*, *AT1G52520.1*, *AUR62013200-AT4G38170.1*, *AUR62002320-AT2G43280.1*, *AT3G59470.2*, *AUR62001611-AT2G27110.1*), indicating that the quinoa *CqFAR1* gene family is more closely related to the *A. thaliana* *FAR1* gene family and may have similar biological functions.

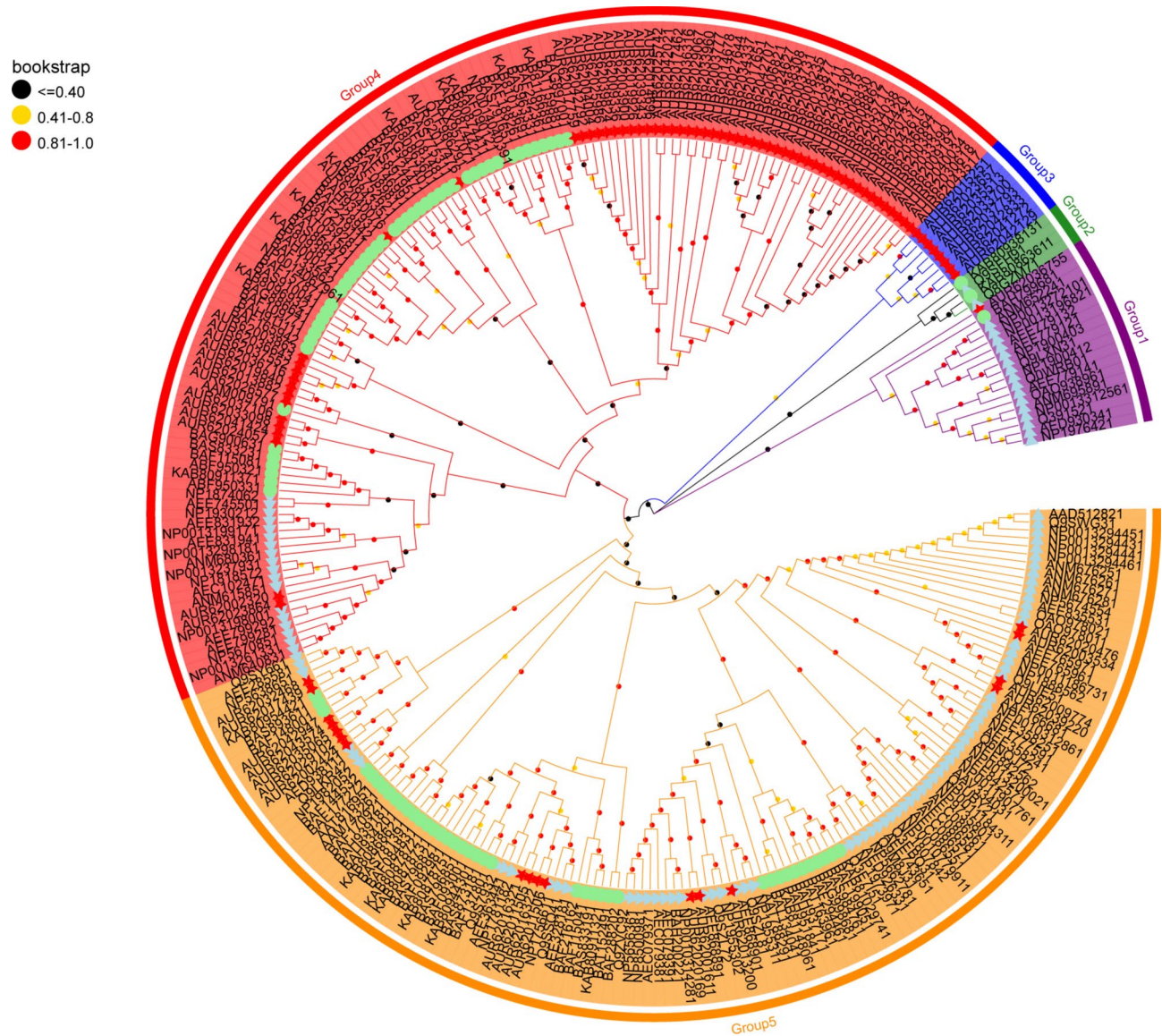


Fig. 1. Phylogenetic tree of the *FAR1* gene family in *C. quinoa*, *A. thaliana* and *O. sativa*. Note: ★, ●, and ▲ indicate the genes of *C. quinoa*, *A. thaliana* and *O. sativa*, respectively. All *FAR1* genes were subdivided into groups I through V; the same branch color represents a group.

Cis acting elements in the promoter region of *CqFAR1* gene

Cis-acting elements are involved in regulating gene expression. We identified 65 cis-regulatory elements in the promoter region of the *CqFAR1* gene family, which were mainly divided into plant hormone elements (abscisic acid response element, salicylic acid response element, gibberellin-response element, cis-acting regulatory element involved in the MeJA-responsiveness, auxin-responsive element); environmental stress elements (cis-acting regulatory element essential for the anaerobic induction, cis-acting element involved in low-temperature responsiveness, cis-acting element involved in defense and stress responsiveness, cis-acting regulatory element involved in circadian control, *MYB* binding site involved in drought-inducibility); photoresponse elements (light responsive element, *MYB* binding site involved in light responsiveness, part of gapA in (gapA-CMA1) involved with light responsiveness); growth and development elements (cis-regulatory element involved in endosperm expression, cis-acting regulatory element involved in seed-specific regulation, AT-rich DNA binding protein (ATBP-1), *MYBHv1* binding site, cis-acting regulatory element related to meristem expression, involved in endosperm-specific negative expression, protein binding site, element involved in differentiation of the palisade mesophyll cells, cis-acting element involved in cell cycle regulation, cis-acting regulatory element root specific, wound-responsive element); secondary metabolic elements (cis-acting regulatory element involved in zein metabolism regulation, *MYB* binding site involved in flavonoid biosynthetic genes regulation) (Fig. 5). Most *CqFAR1* genes exhibit at least one plant hormone response element in their promoter region. Ten cis-acting elements of phytohormone response were identified, including abre, auxrr core, TGA element, TGA box, p-box, gale motif, TatC box, tgacg motif, CGTCA motif, and TCA element. Cis-acting elements play an important role

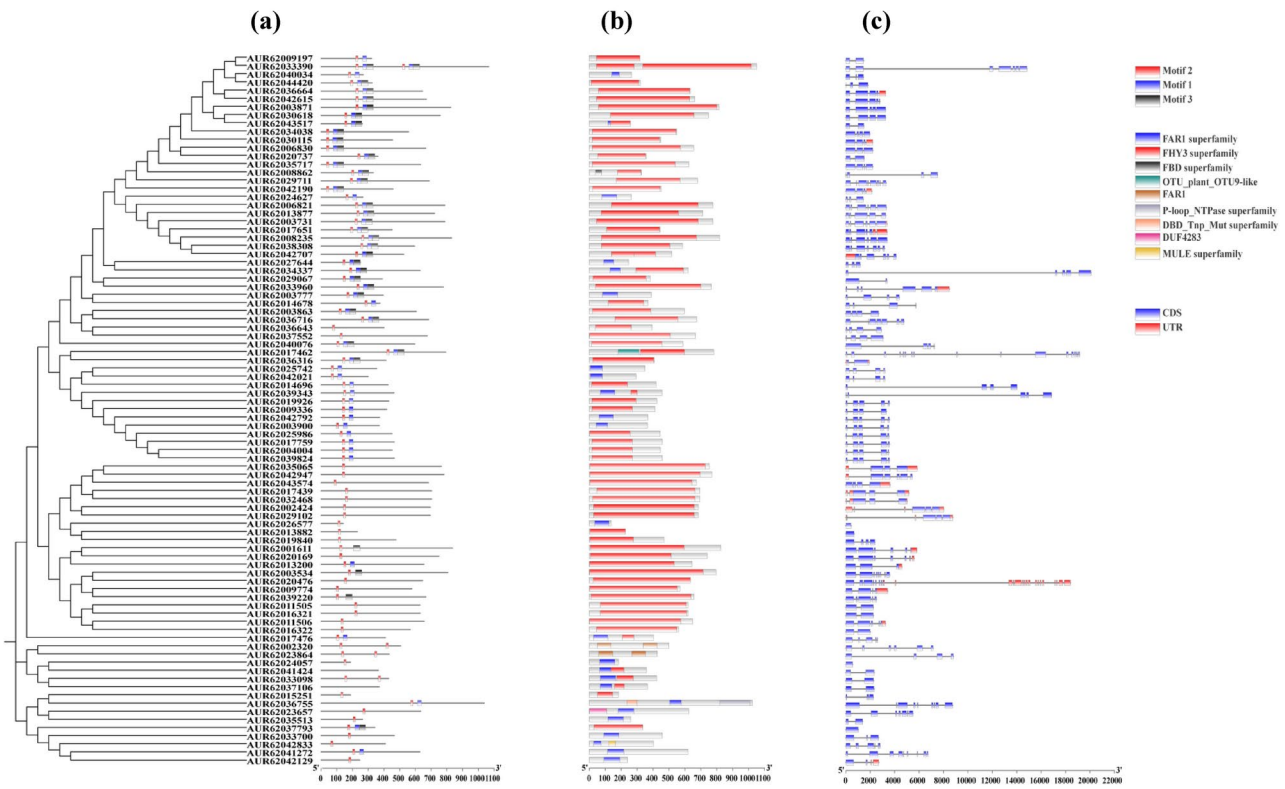


Fig. 2. Protein conserved motif, gene structure and visual analysis of quinoa *CqFAR1* gene family. **(a)** The analysis of conserved motifs in FAR1 proteins. In total, three different motifs are represented by squares of different colors. **(b)** Analysis of protein domains in FAR1 proteins. Various symbols represent different protein structural domains. **(c)** Exon–intron structures of *CqFAR1* genes. Exon–intron structures of *CqFAR1* genes were obtained after analysis with TBtools-II (v2.119) for gene structure. Red bars indicate upstream and downstream UTRs, blue bars indicate coding sequences (CDS), and black lines indicate introns in the gene diagrams.

in regulating the reactivity of ABA, auxin, gibberellin, methyl jasmonate, and salicylic acid. At the same time, the abre homeopathic element is the most common in the *CqFAR1* gene family. In addition, photoresponse elements were present in the promoter region of all *CqFAR1* genes, and 36 cis-acting elements played a role in photoresponse. Six cis-regulatory elements related to abiotic stress response were identified, including LTR, ARE, MBS, TC-rich repeats, circadian, and GC-motif. The root-specific regulatory elements related to growth and development only exist in the gene *AUR62039343*. In addition, the *MYB* binding site was found in *AUR62003863*, *AUR62023657*, and *AUR62044420*, which is an indispensable part of the regulation of flavonoid biosynthesis gene elements. In conclusion, the *CqFAR1* gene family plays an important role in regulating plant growth and development.

GO annotation and functional differentiation of the *CqFAR1* gene family

To understand the function of quinoa *CqFAR1*, we performed GO functional annotation of 87 *CqFAR1* genes, of which 47 *CqFAR1* genes were annotated to biological process (BP), molecular function (MF), and cellular component (CC) categories in the GO database. Among the 47 quinoa *CqFAR1* genes that were functionally annotated, 33 quinoa *CqFAR1* genes were annotated for biological processes, 11 quinoa *CqFAR1* genes for molecular functions, and 3 *CqFAR1* genes for cellular components (Fig. 6a). The GO enrichment bubble plot (Fig. 6b) indicated that the main enrichment was in positive regulation of circadian rhythms, cellular response to far-red light, negative regulation of the developmental process, and other metabolic pathways. These indicate that the *CqFAR1* gene family has functional differentiation and multiple functions in quinoa.

Expression pattern of *CqFAR1* gene

Gene expression patterns provide important clues for understanding potential gene functions. Most *CqFAR1* family members are expressed in all; however, their expression levels in different strains are quite different. Some family members showed preferential expression, and most genes were highly expressed in the control group. Specifically, the expression levels of *AUR62003731* and *AUR62003871* genes were the highest in the control, while the expression levels of *AUR62003777* and *AUR62003863* genes were the highest at 12 h (Fig. 7a). These findings suggest that the *CqFAR1* gene family members have potential roles in growth and development as well as dormancy response. *CqFAR1* genes showed significant expression levels in quinoa spikes, especially the genes

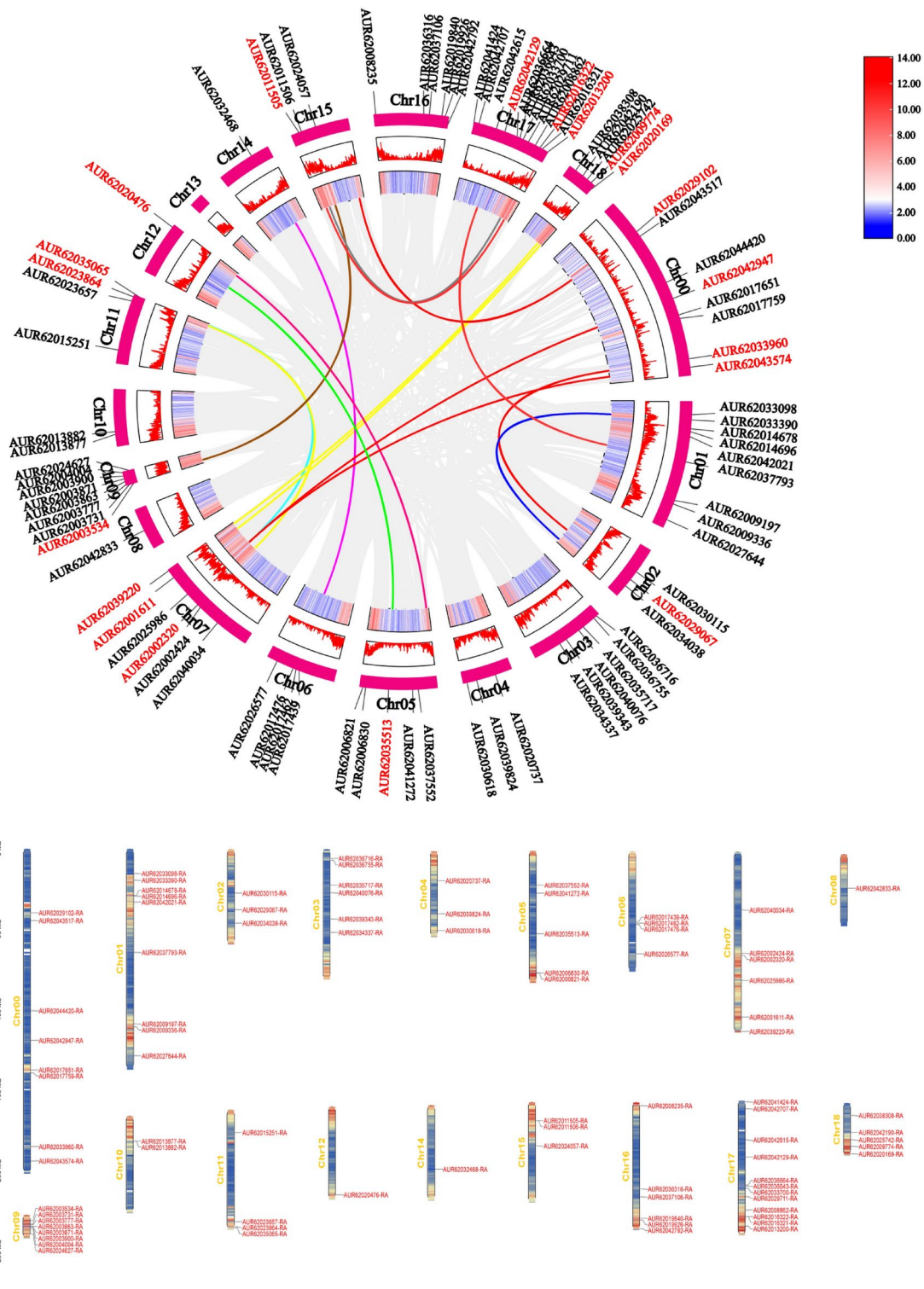


Fig. 3. (a) Location of the *CqFAR1* gene family on quinoa chromosome. (b) Collinear Circos map of the *CqFAR1* gene. Gray lines represent all collinear blocks within the quinoa genome, and colored lines indicate duplicated *CqFAR1* gene pairs.

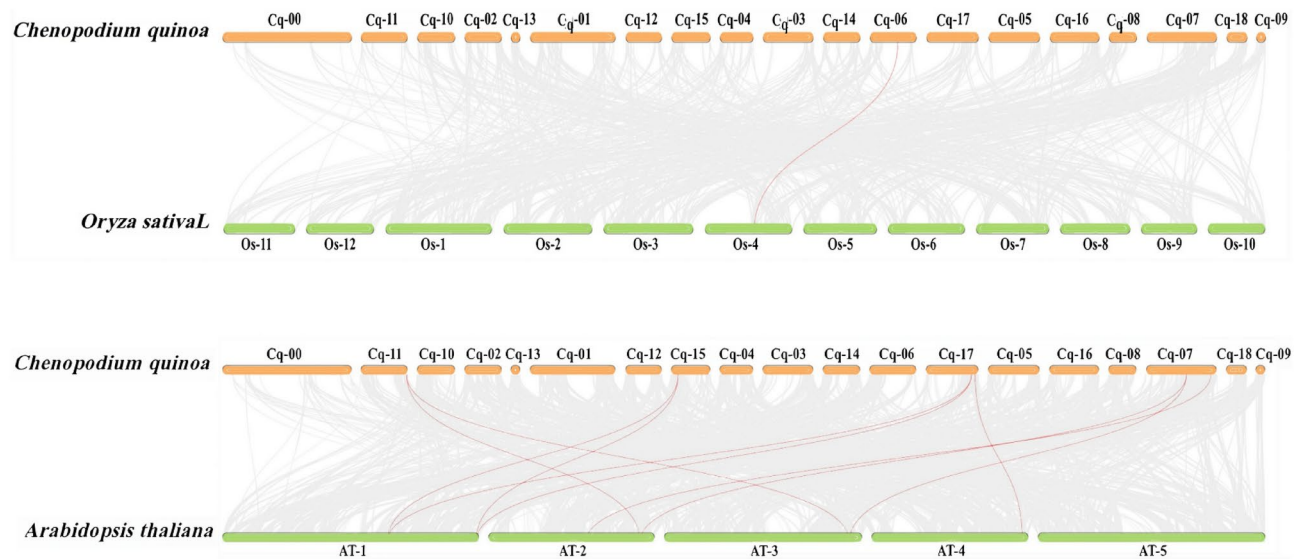


Fig. 4. Analysis of covariance in *C. quinoa*, *O. sativa* and *A. thaliana*.

AUR62003731 and *AUR62003871*. In contrast, the expression of these genes was relatively low in leaves and lowest in quinoa grains. This finding provides important clues for further investigation of the role of *CqFAR1* genes in the growth and development of quinoa (Fig. 7b).

Real-Time Fluorescence Quantitative PCR Validation

To further investigate the effect of the *FAR1* gene on quinoa spike sprouting and to verify the accuracy of the transcriptomic data, we selected six representative *FAR1* genes and five transcriptomic genes in quinoa for real-time fluorescence quantitative analysis (Fig. 8). The results showed that the expression trend of these 11 genes detected by RT-qPCR closely matched the expression trend in the RNA-seq data, proving the reliability of gene expression in this study. The RT-qPCR assay and expression pattern analysis revealed that, except for *AUR62003731* and *AUR62003871*, the expression of the remaining four *CqFAR1* genes was very low in both resistant and sensitive lines, and it was speculated that they were not key regulatory genes. In addition, the decreasing trend of the expression of *AUR62003731* and *AUR62003871* in the sensitive lines was significantly higher than that in the resistant quinoa lines, suggesting that there is some kind of resistance mechanism in the resistant lines, so that the expression of *AUR62003731* and *AUR62003871* can be maintained or only slightly affected. In conclusion, it can be seen that the *FAR1* gene is responsive to quinoa spike sprouting.

Discussion

Gene family analysis reveals the relationship between genetic diversity and functional evolution, providing us with a perspective to deeply understand the role of genes in the adaptive evolution of species²². In this study, we identified 87 *CqFAR1* genes in quinoa, which is significantly more than other crops. This may be due to the combined effect of multiple factors such as quinoa genome size and complexity²³, gene duplication and amplification²⁴, genome doubling events²⁵, and differences in bioinformatics analysis methods²⁶. The quinoa *FAR1* gene is distributed on 18 chromosomes, and 19 pairs of genes have tandem replication and segmental replication, indicating that genome replication events play an important role in maintaining the function of the gene family²⁷. The reason for this analysis may be the high number of quinoa *CqFAR1* gene family members. Based on the subcellular localization of *CqFAR1* family proteins, most of the *CqFAR1* proteins were localized in the cytoplasm. In *O. sativa*, the majority of *OsFAR1* predictions showed that the gene was localized in the cytoplasm²⁸. In *A. thaliana*, the majority of *AtFAR1* predictions showed that the gene was localized in the cytoplasm and endoplasmic reticulum²². The prediction results in quinoa were largely consistent with those in *O. sativa* and *A. thaliana*, and it is hypothesized that the *CqFAR1* gene may perform similar biological functions at the same site in different species. After analysis, it was found that there were some differences in gene structure and motif of different subgroups. They all contain the *FAR1* domain. Phylogenetic tree analysis revealed that quinoa could be divided into five groups, and each group member showed similar exon length and number as well as motif structure. This finding showed that genes belonging to the same group were similar in function.

FAR1 family genes not only have structural diversity, but also may have other functional characteristics. These genes contain a variety of homeopathic elements²⁹, which enable them to respond not only to light signals, but also to the adaptation of quinoa under hypoxia and low temperature conditions and the regulation of circadian rhythm. In addition, the abundant hormone response elements in this family mean that they may play a role in the hormone signal transduction pathway of quinoa. In the promoter region of quinoa *CqFAR1* gene, several cis-regulatory elements have been identified, including GATA element, Box-4 and G-box. These findings suggest that *CqFAR1* gene may be involved in the photosensitive reaction process in quinoa³⁰. There is often a precise regulatory relationship between light reaction and a variety of hormones, which interact with

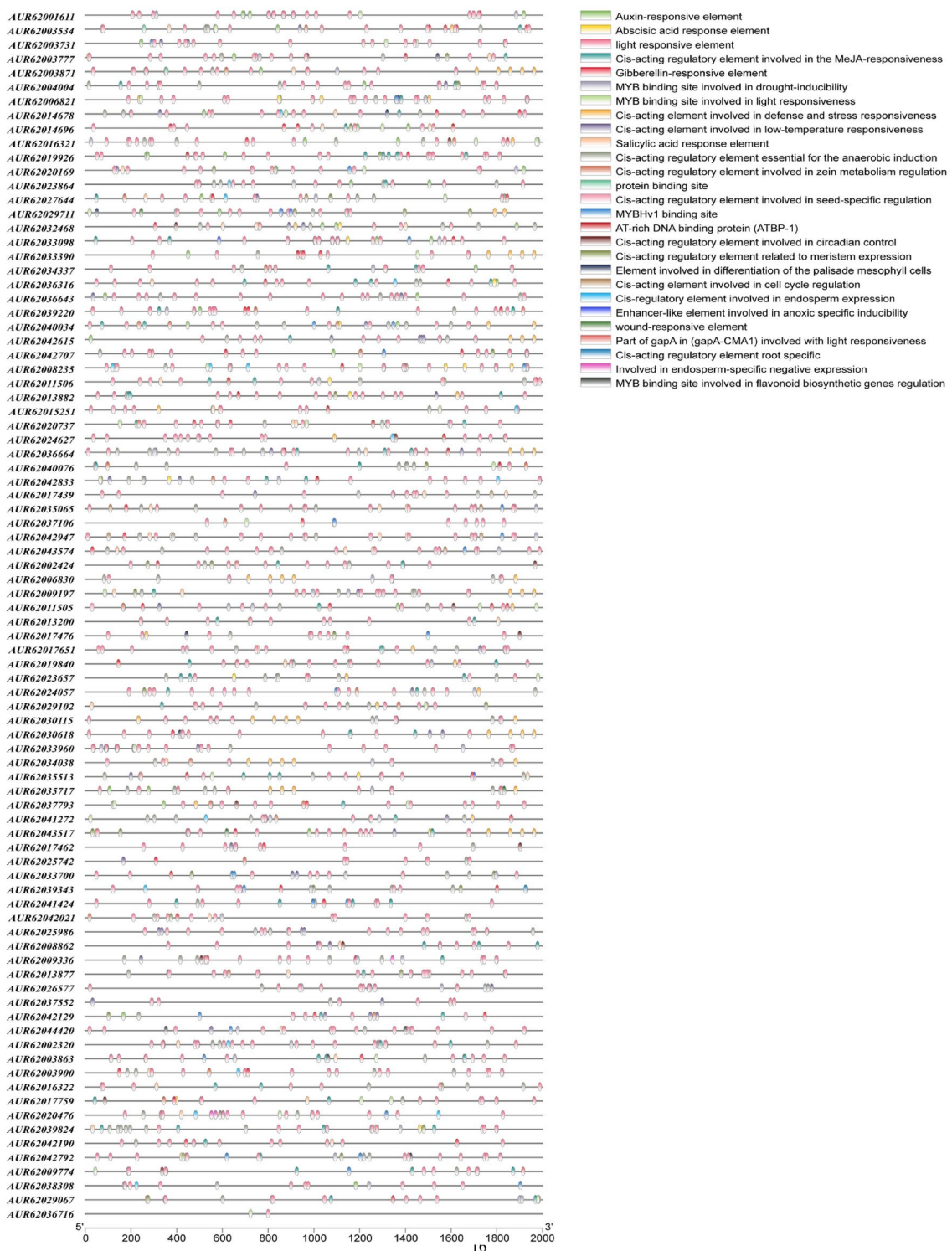


Fig. 5. Cis-acting elements in the *CqFAR1* gene.

each other to maintain physiological balance³. In this study, *CqFAR1* gene, as a positive regulator of ABA signal transduction, has been further revealed. Studies have shown that the promoter of this gene contains multiple response elements, such as ABRE, AUXRR core, TGA element, TGA box and P-box, which may be closely related to ABA synthesis and signal transduction process, indicating that *CqFAR1* plays a key role in the ABA signalling pathway³¹.

Induction of dormancy is a prerequisite for the initiation of dormancy in plants. PhyA, as a major photoreceptor of far-red light, induces the expression of a series of far-red light-responsive genes by transferring them from the cytoplasm to the nucleus, which in turn regulates processes such as seed germination and seedling

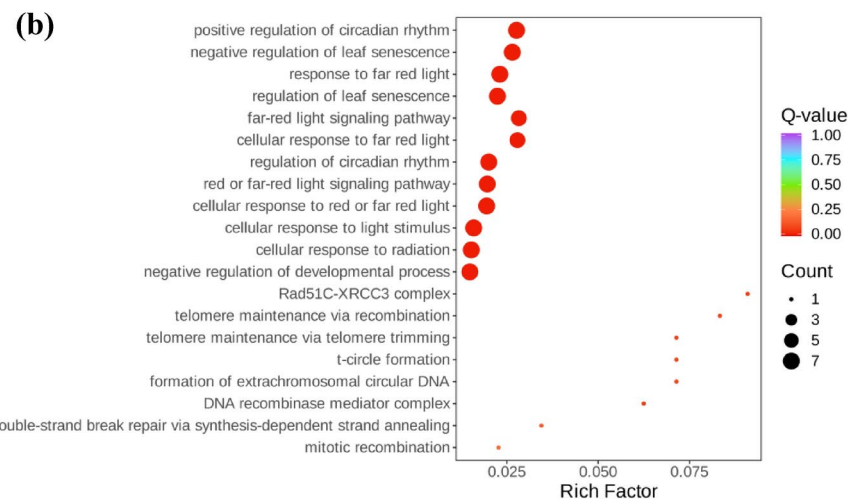
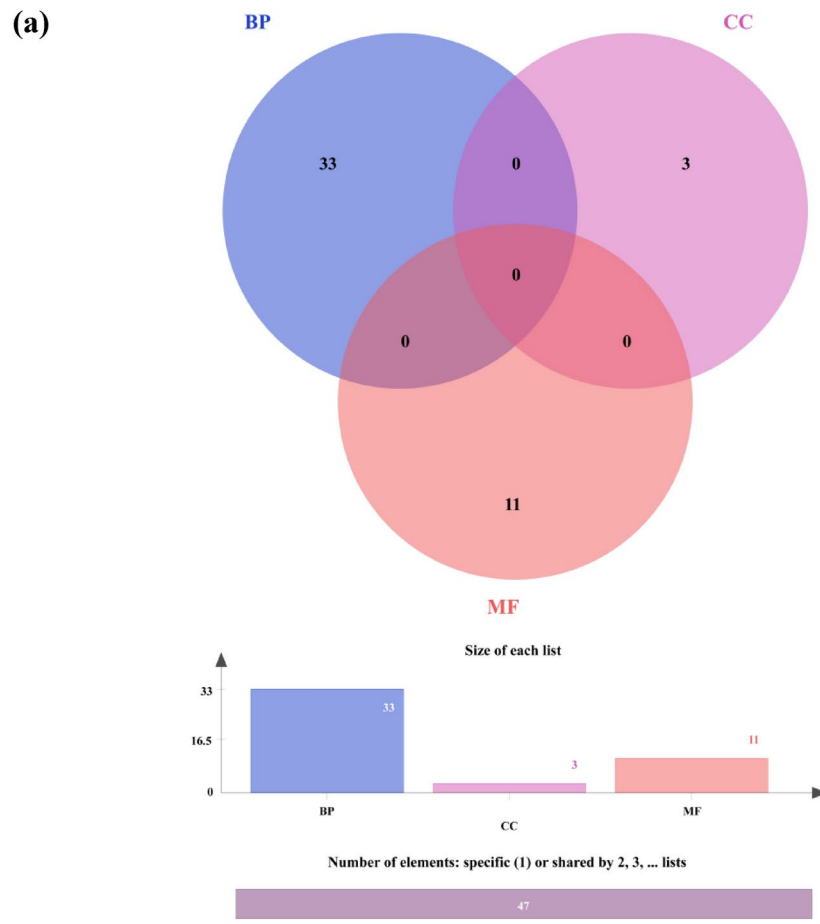


Fig. 6. GO functional annotation and categorization of quinoa *CqFAR1* genes. (a) Venn diagram of quinoa *CqFAR1* genes in the Biological Process (BP), Molecular Function (MF), and Cellular Component (CC) functional categories. (b) GO enrichment bubble diagram.

de-yellowing. In the model plant *A. thaliana*, far-red light significantly down-regulated the expression levels of *FAR1* and *FHY3*⁸. As key regulators in the far-red light pathway, *FAR1* and *FHY3* are not only involved in light signaling but also interact with the abscisic acid (ABA)-related transcription factor *ABI5*, thus linking the light signaling pathway and the hormone signaling pathway, which together affect the dormant state of seeds⁶. It is noteworthy that the expression of *FAR1* and *FHY3* can also be induced by ABA, which further reveals the complex interaction mechanism between light signaling and hormone signaling⁶. In this study, we found that the expression of *AUR62003731* and *AUR62003871* decreased consistently throughout spike sprouting, which

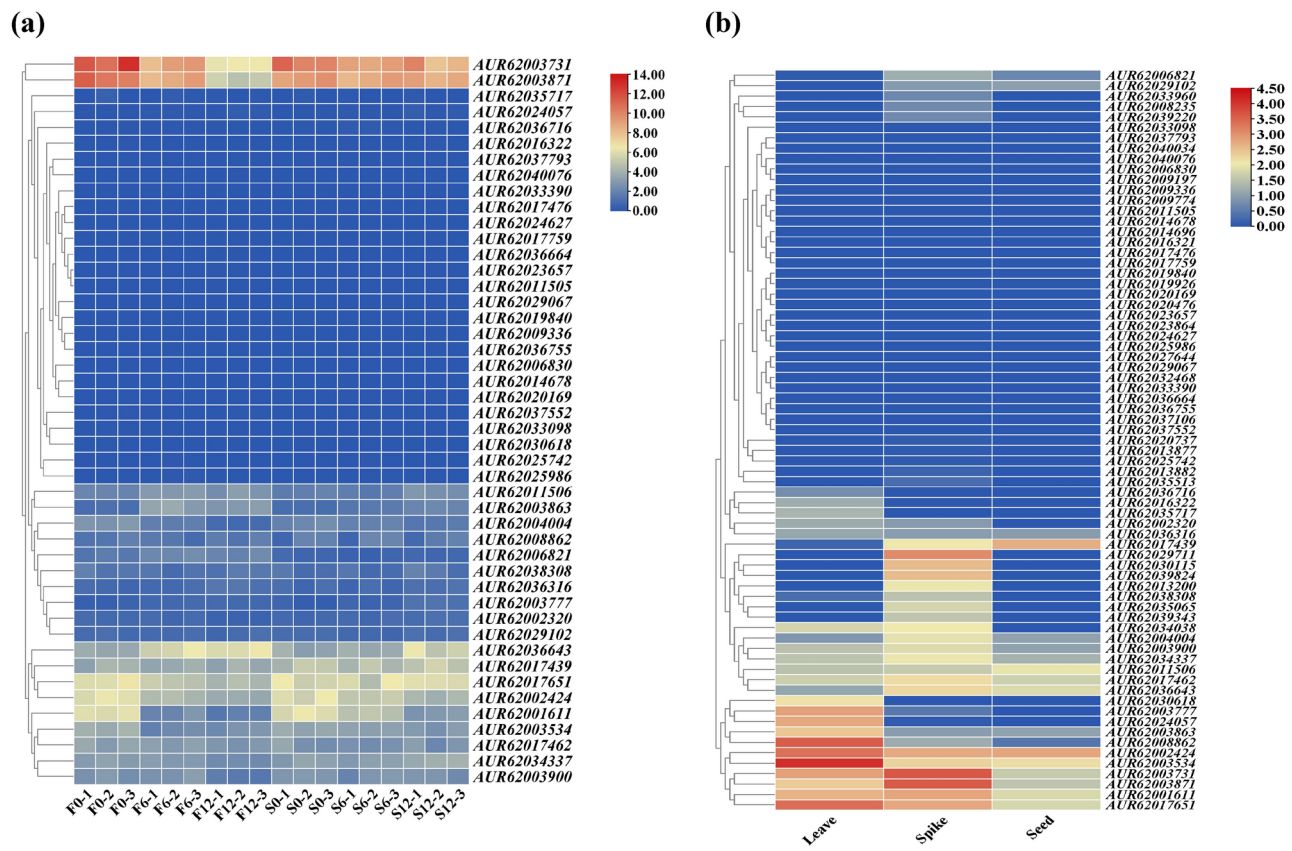


Fig. 7. Heat map of quinoa *CqFAR1* gene expression. **(a)** Expression levels of quinoa *CqFAR1* in different lines at the same time of spike sprouting. **(b)** Expression of quinoa *CqFAR1* gene in different tissues.

may be involved in the induction process of quinoa spike sprouting. In different strains of quinoa, the expression patterns of the *CqFAR1* gene at the same time showed significant differences. In particular, the gene showed a high expression level in the spike of most strains, which suggested that the *CqFAR1* gene might play a key role in the growth and development of the spike. By analyzing the expression patterns of genes, we can predict the physiological activities of these genes to some extent. Previous studies have revealed that in *A. thaliana*, members of the *FAR1* gene family play a key role in regulating flowering timing and growth and development³². In this study, we found that the *CqFAR1* gene had a significant expression pattern in spike tissues. However, the expression of this gene showed a gradual decrease as the spike sprouting process progressed. It is noteworthy that the expression level of *CqFAR1* gene was significantly higher in the sensitive spike sprouting lines compared to the resistant spike sprouting lines. The regulation of the *FAR1* gene on agronomic traits such as spike sprouting has been confirmed in other plants. In *A. thaliana* and *O. sativa*, the *FAR1* gene regulates the synthesis and accumulation of phytochrome by interacting with the FHY1 protein. These genes play a crucial role in the light signal transduction pathway of plants, affecting the perception and adaptation of plants to light conditions^{33,34}. This study showed that the expression level of the *CqFAR1* gene in quinoa panicle was higher than that when the panicle had sprouted, indicating that *CqFAR1* may be involved in regulating the process of panicle germination.

Conclusion

In this study, 87 members of the *CqFAR1* gene family were identified. After examining their physicochemical properties, chromosomal localization, gene organization, evolutionary relationships, and covariance, it was determined that the 87 quinoa *CqFAR1* gene family members were distributed on 18 chromosomes. The *CqFAR1* genes were categorized into five subfamilies, with each subgroup exhibiting the same gene structure and motif. How the quinoa *CqFAR1* gene family is expressed in various tissues and how it responds to spike sprouting was investigated. *AUR62003731* and *AUR62003871* showed significant differences in different quinoa lines and different tissue sites. The findings of this study provide important insights into the evolution of the *CqFAR1* gene family and provide a solid foundation for further exploration of the specific functions of its family members.

Materials and methods

Data source and sequence acquisition of gene family analysis

From ensemblplants³⁵ (<http://plants.ensembl.org/index.html>) download the genome files (cDNA, CDS, DNA.to plevel, PEP) and annotation files (GTF, GFF3) of *C. quinoa* and *O. sativa*. From TAIR (<https://www.arabidopsis.org/>), download the genome and annotation files of *A. thaliana* *FAR1*.

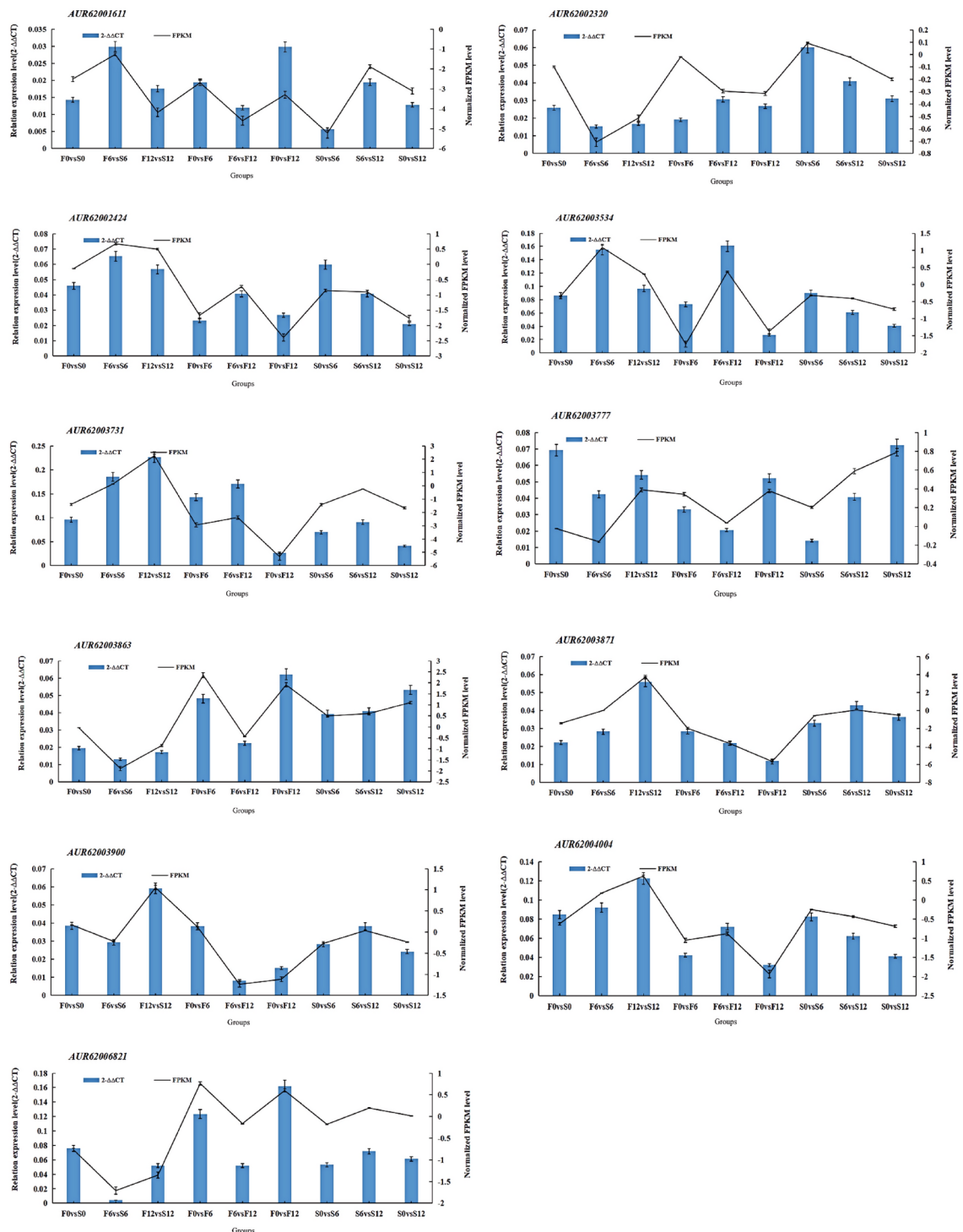


Fig. 8. Validation of the transcription levels for selected DEGs via RT-qPCR.

Gene family identification

To identify all *FAR1* gene family members in *C. quinoa*, first, a TBtools-II (v2.119)³⁶ Blast search (score ≥ 100 , $e \leq 1e^{-10}$) was performed on the genome-wide protein files of *C. quinoa* based on the *A. thaliana* *FAR1* protein sequence to obtain the candidate *FAR1* genes. Second, the hidden Markov model file of the *FAR1* domain (*FAR1*, PF03101) was downloaded from the Pfam database³⁷ (<http://pfam.xfam.org/>), and the HMMER (v3.2.1) program in TBtools-II (v2.119)³⁶ was used to search the whole genome protein of *C. quinoa* to obtain the candidate *FAR1* gene. Third, SMART³⁸ (<http://smart.embl-heidelberg.de/>) and batch CD search³⁹ (<https://www.ncbi.nlm.nih.gov/Structure/cdd/wrpsb.cgi>) were used to domain test all candidate *FAR1* proteins searched by BLAST and HMMER, and each candidate gene was artificially screened to obtain a complete *FAR1* protein.

Finally, the online tool program on the ExPASy⁴⁰ website (<https://web.expasy.org/protparam/>) was used to analyze the physicochemical properties of the FAR1 protein, including protein length, molecular weight, pI, instability index, aliphatic index, grand average hydrophilicity. The Wolf PSORT⁴¹ website (<https://wolfsort.hg.c.jp/>) was used to predict the subcellular localization of the FAR1 protein.

Phylogenetic evolutionary analysis of the *FAR1* gene family in *C. quinoa*

The sequences of the identified FAR1 proteins were subjected to phylogenetic analysis with those of the *A. thaliana* *FAR1* family and *O. sativa* *FAR1* family protein sequences using the built-in Clustal W program in MEGA 7.0 software⁴². The phylogenetic tree was constructed using the neighbor-joining (NJ) method, with the Poisson model selected and the Bootstrap value set to 1,000, the missing values handled by pairwise deletion, and other parameters using the default values. To enhance the visualization, the phylogenetic tree was beautified using EvolView⁴³ (<https://www.evolgenius.info/evolview/>).

Analysis of gene structure and conserved structural domains of the *FAR1* gene family in *C. quinoa*

The MEME Suite online tool⁴⁴ was used to analyze the conserved structural domains of the *CqFAR1* gene family members with the parameter number of motifs set to 3, and the TBtools-II (v2.119)³⁶ software was used to draw the gene structure and motif map. Motif analysis was performed on the protein conservative sequence of each FAR1 (motif number is 3, and the rest is the default). Finally, TBtools-II (v2.119)³⁶ was used to organize and visualize the gene structure of *FAR1* family members.

Chromosome localization and collinearity analysis of the *FAR1* gene family in 5.6 *C. quinoa*

Firstly, this study needs to obtain the gene structure information and chromosomal localization data of the *C. quinoa* FAR1 transcription factor family, which can be extracted from the genome annotation files (GFF3, GTF). In TBtools-II (v2.119)³⁶ software, the “Gene Density Profile” function was used to generate a gene density file, which provided the necessary data support for the mapping of gene localization. Then, the chromosome names and lengths were extracted in “Fasta Tools.” Finally, the “Gene Location Visualization” function was used to visualize the gene locations.

Chenopodium quinoa *FAR1* gene family duplicates were identified based on the following criteria: (1) coverage of the shorter gene sequence length was greater than 70% of the longer sequence; and (2) similarity was greater than 70% when comparing the two sequences. Two genes of the same family that are five or fewer genes apart in a 100 kb chromosome segment are considered tandem duplications^{45,46}. Next, to deeply understand the evolutionary relationship of *FAR1* family genes, this study analyzed the collinearity of *FAR1* family genes in *C. quinoa*, *A. thaliana*, and *O. sativa* using the MCScanX algorithm in TBtools-II (v2.119)³⁶. Subsequently, the visualization tools in TBtools-II (v2.119)³⁶ were used to intuitively display the analysis results to facilitate the comparison and interpretation of the collinearity evolution patterns of *FAR1* family genes among different species.

Analysis of promoter *cis*-acting elements of the *CqFAR1* gene family in *C. quinoa*

First, we extracted all upstream sequences (2000 bp) of the quinoa *FAR1* gene family and uploaded them to the PlantCARE⁴⁷ database (<https://bioinformatics.psb.ugent.be/webtools/plantcare/html/>). After manually screening for relevant *cis*-acting elements, we mapped them using the TBtools-II (v2.119)³⁶ software.

GO annotation and functional classification of the *FAR1* gene family in quinoa

Blast2Go version 5.0⁴⁸ was used to annotate and classify *FAR1* transcripts. According to the annotation results, these transcripts were divided into different functional categories (biological process, molecular function, and cellular composition), and the number of transcripts under each functional category was counted. The results were visualized using the online tool jvnn (<https://jvnn.toulouse.inrae.fr/app/example.html>)⁴⁹.

Analysis of plant materials, growth conditions, treatments, and tissue site expression patterns

It was planted in Xundian County, Kunming City, Yunnan Province (102°41'E, 25°20'N, 1766 m above sea level) and harvested immediately after 120 days of maturity using conventional management and normal fertilization. Since quinoa spikes had more seeds and were covered with sepals, which were difficult to observe, one spikelet was randomly selected from the main spike of quinoa and clipped for the experiment. Two quinoa lines, sensitive (Dianli-222) and resistant (Dianli-654), were selected. Distilled water was sprayed regularly to provide a moist environment for quinoa. When determining spike sprouting, the number of seeds was observed and counted every 6 h. The results showed that the sensitive strain partially germinated at 6 h, the resistant strain showed no sprouting, and the difference was greatest at 12 h, which was the optimal sampling time for both strains (0/6/12 h). A total of 18 samples with three biological replicates were frozen in liquid nitrogen and stored in a – 80 °C refrigerator for subsequent transcriptome sequencing analysis. The experimental process of transcriptome sequencing includes RNA extraction, RNA detection, library construction, and online sequencing. The downstream data will be filtered to obtain clean data, and then compared with the specified reference genome to obtain mapped data, which will be used to perform structural level analyses such as variable splicing analysis, new gene discovery, and gene structure optimization, etc. According to the expression of the genes in different samples or different sample groups, we will carry out expression level analyses such as differential expression analysis, differentially expressed gene function annotation, and function enrichment analysis. We used FPKM (Fragments Per Kilobase of transcript per Million fragments mapped) as a measure of the expression level of transcripts or genes, and screened differential genes with $|\log_2 \text{Fold Change}| \geq 1$ and

FDR<0.05. We used RNA-seq data (<https://www.ncbi.nlm.nih.gov/sra/SP474959>), including sensitive and resistant material, corresponding to three periods. We analyzed the transcript levels of the *FARI* gene family in different strains during the same period and used TBtools-II (v2.119)³⁶ to create a heat map of gene expression (v2.119). In addition, leaf, seed, and spike transcriptome sequencing data of quinoa were downloaded from the NCBI SRA database (<http://www.ncbi.nlm.nih.gov/sra/>) under the sequence numbers SRP383884, SRP474959, and SRP431581, respectively. Based on the above data, the transcriptome sequencing data of *C. quinoa* were analyzed using Tophat⁵⁰ and Cufflink⁵¹ software packages to analyze the transcriptome sequencing data and perform expression calculations to extract the gene expression data of the *FARI* gene family members. The expression data were normalized, and the expression heatmaps created using TBtools-II (v2.119)³⁶ software illustrated the expression patterns of the *C. quinoa FARI* gene family in various tissues.

Presentation of RNA and establishment of cDNA libraries

In this experiment, the CTAB method was used to extract RNA⁵². The kit used was the Hieff NGS® Ultima Dual-mode mRNA Library Prep Kit. The library construction process included: total starting RNA \geq 1 μ g, enrichment of mRNA and fragmentation using Oligo(dT) magnetic beads; synthesis of the first strand of cDNA by M-MuLV reverse transcriptase, and synthesis of the second strand by RNase H degradation of RNA; after double-stranded cDNA was end-repaired, A-tailed ligated and ligated with sequencing junctions, the cDNA library was screened, PCR-amplified and purified. The cDNA library was initially quantified and diluted to 1.5 ng/ μ L using Qubit 2.0, the insert size was measured by Agilent 2100, and the effective concentration (> 2 nM) was accurately quantified by qRT-PCR to ensure the quality.

Real-time fluorescence quantitative PCR validation

To verify the reliability of the transcriptome sequencing results, the *FARI*-related genes with high expression in the transcriptome were selected for RT-qPCR experiments. The *ACT-1* gene was chosen as an internal reference gene and primers for the associated gene were designed in Beacon Designer 7.9 for RT-qPCR analysis^{53,54}. The PerfectStart SYBR qPCR supermix (TransGen Biotech, Beijing, China) was used for RT-qPCR according to the manufacturer's instructions. The reaction volume was 20 μ L, including 2 \times Perfectstart™ SYBR qPCR Supermix 10 μ L, calibration solution 0.4 μ L, nuclease-free water (RNase-free water) 6.8 μ L, forward primer and reverse primer each (10 μ M) 0.4 μ L, cDNA 2 μ L (200 ng/ μ L). The thermal cycle was as follows: 94 °C (30 s), 94 °C (5 s), 60 °C (30 s), for 40 cycles. The relative gene expression level was calculated using the $2^{-\Delta\Delta CT}$ method⁵⁵.

Data availability

The original contributions presented in the study are publicly available. This data can be found here National Center for Biotechnology Information (NCBI) SRA database under accession number a SRP474959. The names of the repository and accession number(s) can be found below: <https://www.ncbi.nlm.nih.gov/sra/SP474959>.

Received: 4 August 2024; Accepted: 10 November 2024

Published online: 18 November 2024

References

1. Wang, H. & Wang, H. Multifaceted roles of FHY3 and FAR1 in light signaling and beyond. *Trends Plant Sci.* **20**, 453–461 (2015).
2. Jiang, Y. et al. Genome-wide identification and integrated analysis of the FARI/FHY3 gene family and genes expression analysis under methyl jasmonate treatment in Panax Ginseng C A. Mey. *BMC Plant Biol.* **24**, 549 (2024).
3. Xie, Y. et al. Arabidopsis FHY3 and FAR1 integrate light and strigolactone signaling to regulate branching. *Nat. Commun.* **11**, 1955 (2020).
4. Wang, H. & Deng, X. W. Arabidopsis FHY3 defines a key phytochrome a signaling component directly interacting with its homologous partner FAR1. *Embo J.* **21**, 1339–1349 (2002).
5. McCormac, A. C. & Terry, M. J. Light-signalling pathways leading to the co-ordinated expression of HEMA1 and Lhcb during chloroplast development in arabidopsis Thaliana. *Plant J.* **32**, 549–559 (2002).
6. Tang, W. et al. FAR-RED elongated HYPOCOTYL3 and FAR-RED IMPAIRED RESPONSE1 transcription factors integrate light and abscisic acid signaling in arabidopsis. *Plant Physiol.* **163**, 857–866 (2013).
7. Li, G. et al. Coordinated transcriptional regulation underlying the circadian clock in arabidopsis. *Nat. Cell Biol.* **13**, 616–622 (2011).
8. Lin, R. et al. Transposase-derived transcription factors regulate light signaling in arabidopsis. *Science.* **318**, 1302–1305 (2007).
9. Ouyang, X. et al. Genome-wide binding site analysis of FAR-RED ELONGATED HYPOCOTYL3 reveals its novel function in arabidopsis development. *Plant Cell.* **23**, 2514–2535 (2011).
10. Ma, L., Xue, N., Fu, X., Zhang, H. & Li, G. Arabidopsis Thaliana FAR-RED ELONGATED HYPOCOTYL3 (FHY3) and FAR-RED-IMPAIRED RESPONSE1 (FAR1) modulate starch synthesis in response to light and sugar. *New Phytol.* **213**, 1682–1696 (2017).
11. Dai, J. et al. FAR1/FHY3 transcription factors positively regulate the salt and temperature stress responses in eucalyptus grandis. *Front. Plant Sci.* **13**, 883654 (2022).
12. Lu, Q. et al. Genome-wide identification and expression of FAR1 gene family provide insight into pod development in peanut (*Arachis hypogaea*). *Front. Plant Sci.* **13**, 893278 (2022).
13. Tang, H. et al. Genome-wide identification and expression analyses of the FARI/FHY3 gene family provide insight into inflorescence development in maize. *Curr. Issues Mol. Biol.* **46**, 430–449 (2024).
14. Chen, Q. et al. Genome-wide identification and functional characterization of FAR1-RELATED SEQUENCE (FRS) family members in potato (*Solanum tuberosum*). *Plants (Basel)* **12**, (2023).
15. Liang, Y., Liu, H. J., Yan, J. & Tian, F. Natural variation in crops: Realized understanding, continuing promise. *Annu. Rev. Plant Biol.* **72**, 357–385 (2021).
16. Park, M., Shin, S. Y., Moon, H., Choi, W. & Shin, C. Analysis of the global transcriptome and miRNAome associated with seed dormancy during seed maturation in rice (*Oryza Sativa L. Cv. Nipponbare*). *BMC Plant Biol.* **24**, 215 (2024).
17. Lee, C. M. et al. QTL mapping and improvement of pre-harvest sprouting resistance using japonica weedy rice. *Front. Plant Sci.* **14**, 1194058 (2023).

18. Ozcaliskan, I. H. et al. Quinoa (*Chenopodium Quinoa* Willd) supplemented cafeteria diet ameliorates glucose intolerance in rats. *Food Sci Nutr.* **11**, 6920–6930 (2023).
19. Ain, Q. T. et al. Adaptive mechanisms in quinoa for coping in stressful environments: An update. *PeerJ.* **11**, e14832 (2023).
20. Shen, Z. J. et al. TMT proteomics analysis of a pseudocereal crop, quinoa (*Chenopodium Quinoa* Willd) during seed maturation. *Front. Plant Sci.* **13**, 975073 (2022).
21. Matias, J. et al. Assessment of the changes in seed yield and nutritional quality of quinoa grown under rainfed mediterranean environments. *Front. Plant Sci.* **14**, 1268014 (2023).
22. Lin, R. & Wang, H. Arabidopsis FHY3/FAR1 gene family and distinct roles of its members in light control of arabidopsis development. *Plant Physiol.* **136**, 4010–4022 (2004).
23. Bennett, M. D. & Leitch, I. J. Nuclear DNA amounts in angiosperms: Targets trends and tomorrow. *Ann Bot.* **107**, 467–590 (2011).
24. Van de Peer, Y., Maere, S. & Meyer, A. The evolutionary significance of ancient genome duplications. *Nat. Rev. Genet.* **10**, 725–732 (2009).
25. Wendel, J. F., Jackson, S. A., Meyers, B. C. & Wing, R. A. Evolution of plant genome architecture. *Genome Biol.* **17**, 37 (2016).
26. Li, L., Stoeckert, C. J. & Roos, D. S. OrthoMCL: Identification of ortholog groups for eukaryotic genomes. *Genome Res.* **13**, 2178–2189 (2003).
27. Kong, H. et al. Patterns of gene duplication in the plant SKP1 gene family in angiosperms: Evidence for multiple mechanisms of rapid gene birth. *Plant J.* **50**, 873–885 (2007).
28. Zhou, D. et al. Characterization of the fatty Acyl-CoA reductase (FAR) gene family and its response to abiotic stress in rice (*Oryza sativa* L.). *Plants (Basel)*. **13**, (2024).
29. Marand, A. P., Eveland, A. L., Kaufmann, K. & Springer, N. M. Cis-regulatory elements in plant development, adaptation, and evolution. *Annu. Rev. Plant Biol.* **74**, 111–137 (2023).
30. Baek, K. et al. Introducing *dunaliella* LIP promoter containing light-inducible motifs improves transgenic expression in chlamydomonas reinhardtii. *Biotechnol. J.* **11**, 384–392 (2016).
31. Wang, X. et al. ABRE-BINDING FACTORS play a role in the feedback regulation of aba signaling by mediating rapid ABA induction of ABA co-receptor genes. *New Phytol.* **221**, 341–355 (2019).
32. Ritter, A. et al. The transcriptional repressor complex FRS7-FRS12 regulates flowering time and growth in arabidopsis. *Nat. Commun.* **8**, 15235 (2017).
33. Feng, Z. J. et al. Foxtail millet NF-Y families: Genome-wide survey and evolution analyses identified two functional genes important in abiotic stresses. *Front. Plant Sci.* **6**, 1142 (2015).
34. Wang, W. et al. A pair of light signaling factors FHY3 and FAR1 regulates plant immunity by modulating chlorophyll biosynthesis. *J. Integr. Plant Biol.* **58**, 91–103 (2016).
35. Cunningham, F. et al. Ensembl 2022. *Nucleic Acids Res.* **50**, D988–D995 (2022).
36. Chen, C. et al. TBtools-II: A “One for All, All for One” bioinformatics platform for biological big-data mining. *Mol. Plant.* **16**, 1733–1742 (2023).
37. Blum, M. et al. The InterPro protein families and domains database: 20 years on. *Nucleic Acids Res.* **49**, D344–D354 (2021).
38. Letunic, I. & Bork, P. 20 years of the SMART protein domain annotation resource. *Nucleic Acids Res.* **46**, D493–D496 (2018).
39. Lu, S. et al. CDD/SPARCLE: The conserved domain database in 2020. *Nucleic Acids Res.* **48**, D265–D268 (2020).
40. Wilkins, M. R. et al. Protein identification and analysis tools in the ExPASy server. *Methods Mol Biol.* **112**, 531–552 (1999).
41. Horton, P. et al. WoLF PSORT: Protein localization predictor. *Nucleic Acids Res.* **35**, W585–W587 (2007).
42. Tamura, K., Stecher, G. & Kumar, S. MEGA11: Molecular evolutionary genetics analysis version 11. *Mol. Biol. Evol.* **38**, 3022–3027 (2021).
43. Subramanian, B., Gao, S., Lercher, M. J., Hu, S. & Chen, W. H. Evolview V3: A webserver for visualization, annotation, and management of phylogenetic trees. *Nucleic Acids Res.* **47**, W270–W275 (2019).
44. Bailey, T. L. et al. MEME SUITE: Tools for motif discovery and searching. *Nucleic Acids Res.* **37**, W202–W208 (2009).
45. Gu, Z., Cavalcanti, A., Chen, F. C., Bouman, P. & Li, W. H. Extent of gene duplication in the genomes of drosophila, nematode, and yeast. *Mol. Biol. Evol.* **19**, 256–262 (2002).
46. Yang, S., Zhang, X., Yue, J. X., Tian, D. & Chen, J. Q. Recent duplications dominate NBS-encoding gene expansion in two woody species. *Mol. Genet. Genomics.* **280**, 187–198 (2008).
47. Lescot, M. et al. PlantCARE, a database of plant cis-acting regulatory elements and a portal to tools for in silico analysis of promoter sequences. *Nucleic Acids Res.* **30**, 325–327 (2002).
48. Conesa, A. et al. Blast2GO: A universal tool for annotation, visualization and analysis in functional genomics research. *Bioinformatics.* **21**, 3674–3676 (2005).
49. Bardou, P., Mariette, J., Escudie, F., Djemiel, C. & Klopp, C. Jvenn: An interactive Venn diagram viewer. *BMC Bioinformatics.* **15**, 293 (2014).
50. Trapnell, C., Pachter, L. & Salzberg, S. L. TopHat: Discovering splice junctions with RNA-Seq. *Bioinformatics.* **25**, 1105–1111 (2009).
51. Trapnell, C. et al. Differential gene and transcript expression analysis of RNA-seq experiments with TopHat and Cufflinks. *Nat. Protoc.* **7**, 562–578 (2012).
52. Mainkar, P. et al. Development of Modified CTAB and trizol protocols to isolate high molecular weight (HMW) RNA from polyphenol and polysaccharides rich pigeonea (*Cajanus cajan* (L.) Millsp). *PLoS One.* **18**, e291949 (2023).
53. Tian, C. et al. Selection of suitable reference genes for qPCR normalization under abiotic stresses and hormone stimuli in carrot leaves. *PLoS One.* **10**, e117569 (2015).
54. Chen, C. et al. Identification of reliable reference genes for quantitative real-time PCR Normalization in Pitaya. *Plant Methods.* **15**, 70 (2019).
55. Livak, K. J. & Schmittgen, T. D. Analysis of relative gene expression data using real-time quantitative PCR and the 2(-Delta Delta C(T)) method. *Methods.* **25**, 402–408 (2001).

Acknowledgements

We wish to acknowledge the Wuhan Metware Biotechnology Co., Ltd., for Professional technical services. We also thank professor Peng Qin conducted with the experiments for their valuable help and guidance.

Author contributions

LBH wrote the original draft and performed the methodology. LYZ wrote the original draft and carried out the formal analysis. PZ did the conceptualization, and wrote, reviewed, and edited the manuscript. JNL carried out the formal analysis, performed the methodology, and visualized the data. LL collected the field samples and prepared the plant materials. HXL carried out the formal analysis and investigated the data. XQW and YTB and GFJ carried out the formal analysis and investigated the data. PQ supervised the data and carried out the project administration and funding acquisition. All authors contributed to the article and approved the submitted version.

Funding

We gratefully acknowledge the financial support of the Academician Expert Workstation (202405AF140012) and the Yunnan Expert Workstation (202205AF150001) and the “Xingdian Talent” Industry Innovation Talent Program in Yunnan Province (XDYCCYCX-2022-0029).

Declarations

Competing interests

The authors declare no competing interests.

Additional information

Correspondence and requests for materials should be addressed to P.Q.

Reprints and permissions information is available at www.nature.com/reprints.

Publisher’s note Springer Nature remains neutral with regard to jurisdictional claims in published maps and institutional affiliations.

Open Access This article is licensed under a Creative Commons Attribution-NonCommercial-NoDerivatives 4.0 International License, which permits any non-commercial use, sharing, distribution and reproduction in any medium or format, as long as you give appropriate credit to the original author(s) and the source, provide a link to the Creative Commons licence, and indicate if you modified the licensed material. You do not have permission under this licence to share adapted material derived from this article or parts of it. The images or other third party material in this article are included in the article’s Creative Commons licence, unless indicated otherwise in a credit line to the material. If material is not included in the article’s Creative Commons licence and your intended use is not permitted by statutory regulation or exceeds the permitted use, you will need to obtain permission directly from the copyright holder. To view a copy of this licence, visit <http://creativecommons.org/licenses/by-nc-nd/4.0/>.

© The Author(s) 2024